

Ethylene-Triggered Formation of Ruthenium Alkylidene from Decomposed Catalyst

Wietse Smit,[‡] Marco Foscatto,^{*,‡} Giovanni Occhipinti,^{*} and Vidar R. Jensen^{*}

Department of Chemistry, University of Bergen, Allégaten 41, N-5007 Bergen, Norway

KEYWORDS: ruthenium, alkylidene, ethylene, olefin metathesis, catalyst decomposition, N-heterocyclic carbene.

Supporting Information Placeholder

ABSTRACT: Ethylene is known to readily decompose ruthenium-based olefin metathesis catalysts, such as Grubbs second-generation catalyst (**GII**), by forming the unsubstituted ruthenacyclobutane (**Ru-2**) that may undergo a 1,2-H shift and liberate propene. The resulting alkylidene loss has been assumed to be irreversible. Yet, by reacting $\text{RuCl}_2(\text{SIMes})(p\text{-cymene})$ (**1**), the *p*-cymene-stabilized alkylidene-free fragment resulting from loss of propene from **Ru-2**, with ethylene, we show that the methylidene-analogue of **GII** (**GIIIm**) and other Ru alkylidenes are formed, along with catalytic amounts of propene and butenes, and can be stabilized by tricyclohexylphosphine (PCy_3) at 50 °C in C_6D_6 . An almost 20-fold increase in activity for ring-closing metathesis of DEDAM on pretreatment of **1** with ethylene suggests that the reversibility of the alkylidene loss may be used to develop longer-lived metathesis catalysts and processes. Mechanistic DFT calculations suggest that the connection between **1** and **GIIIm** involves oxidative coupling of two ethylene molecules to form a key metallacyclopentane intermediate (**M49**). A 1,2-H shift in **M49** gives the methyl-substituted ruthenacyclobutane **M303**, which, on cycloreversion, liberates propene and **GIIIm**. Alternatively, successive H-shifts starting in **M49** may give 1-butene (fast reaction) and 2-butene (slower) with a lower barrier than that of Ru alkylidene. The lower predicted barrier is consistent with butene, especially 1-butene, being the dominating product at the start of the experiments, in particular at lower temperature.

INTRODUCTION

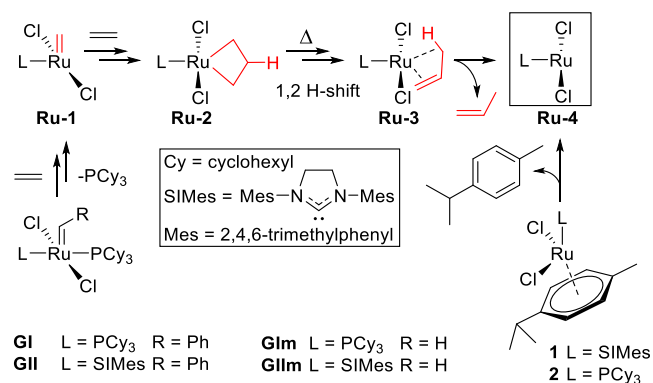
Although olefin metathesis has evolved to become one of the broadest applicable catalytic technologies for the assembly of carbon-carbon bonds,¹ popular, functional group tolerant, and easy-to-handle ruthenium-based catalysts such as Grubbs second-generation catalyst (**GII**, Scheme 1)² suffer from a vulnerability that limits their further industrial uptake in valorization of renewable feedstocks and production of natural products and pharmaceuticals:³⁻⁶ the low stability of the key catalytic intermediates, which typically results in catalyst decomposition after only a few thousand turnovers.⁷⁻¹¹ Particularly rapid decomposition is observed with ethylene as substrate¹²⁻¹⁴ which so far has precluded the use of this, the smallest and most atom-economic coupling partner in metathesis “cracking” of unsaturated plant oils.^{4,15-17}

Ethylene as a metathesis partner initiates decomposition of the otherwise robust catalyst precursors such as **GI** and **GII**

(Scheme 1) by frequently forming the key vulnerable intermediates **Ru-1**, the Ru methylidene, and **Ru-2**, the unsubstituted ruthenacyclobutane. While **Ru-1** is susceptible to methylidene abstraction, by free PCy_3 generated upon initiation of **GII** or **GIIIm**,^{18,19} or *via* a Buchner ring expansion triggered by π -acids,^{20,21} **Ru-2** may readily undergo β -hydrogen transfer to form an allyl-hydride species, followed by elimination of propene *via* an overall 1,2-H shift (Scheme 1). First observed in Mo-based metathesis,²² metallacyclobutane decomposition *via* 1,2-H shift and propene elimination is now well established for early transition-metals catalysts,²³⁻²⁵ and, thanks to mechanistic investigations involving experimental²⁶⁻²⁹ and molecular-level computational methods^{26,28,30-32} also for ruthenium-based catalysts.²⁴

Decomposition *via* the overall 1,2-H shift depicted in Scheme 1 leads to the propene-coordinated Ru complex **Ru-3**. The latter contains a highly electron deficient and reactive alkylidene-free Ru fragment **Ru-4** (formed by removal of propene) that easily undergoes cyclometalation of the SIMes ligand,^{13,33} coordinates and isomerizes olefins,³¹ and which may likely also aggregate to form Ru nanoparticles (RuNPs).³⁴

Scheme 1. Decomposition of the Unsubstituted Ruthenacyclobutane **Ru-2** *via* 1,2-H Shift.^a



^a β -hydride elimination in **Ru-2** gives a Ru-allyl-hydride intermediate (not shown). Next, hydride transfer to the terminal allyl methylene results in **Ru-3**. **Ru-4** may also result from dissociation of *p*-cymene from **1** or **2**.

Despite its reactivity and role in secondary decomposition reactions, **Ru-4** may be “trapped” and isolated by donor stabilization^{13,35} during decomposition of second-generation catalysts such as **GII** and **GIIIm**. Even though ruthenium

alkylidenes may be formed on treatment of donor-stabilized versions of **Ru-4** (**1**, **2**, and analogues thereof) with highly reactive carbene initiators such as diazomethanes^{36,37} and propargyl alcohols,^{38,39} the decomposition of catalysts such as **GII** and **GIIIm** has been assumed to be irreversible.²⁴ Here, we show, for the first time, that the reverse reaction, formation and donor-stabilization of Ru alkylidenes, is possible without carbene initiators, simply by treatment of donor-stabilized **Ru-4** with the olefin known to be the most threatening to the stability of metathesis catalysts, namely ethylene.

RESULTS AND DISCUSSION

Alkylidene Formation from 1 And Ethylene. Although ethylene reduces the stability of any Ru alkylidene formed, this substrate also facilitates alkylidene observation and analysis of the reaction mixture by not isomerizing *via* double-bond migration and by being invisible in self-metathesis. We were also encouraged by the early observation that decomposition of **GIIIm** in the presence of ethylene (as in Scheme 1) led to more propene than the equivalent of decomposed catalyst,²⁶ and started by reacting **1** with excess ethylene in C₆D₆ at 25 °C. The mixture was protected from light in an NMR tube with minimal headspace, and the reaction was followed by recording a ¹H NMR spectrum every 30 min; see Supporting Information for details. As shown in Figure 1, the ¹H NMR spectra revealed the presence of butenes (1-butene as well as *cis*- and *trans*-2-butene), ethane, and, importantly, propene.⁴⁰ Propene is likely to originate from ethenolysis of 2-butene (Scheme 2) and from decomposition of **Ru-2** *via* Scheme 1, and is a known indicator of ruthenium alkylidene.

Scheme 2. Generation of Propene *via* Ethenolysis of *cis*- and *trans*-2-Butene.

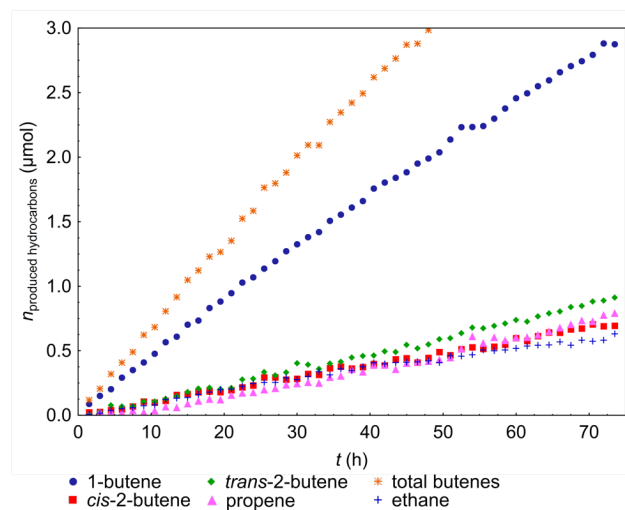
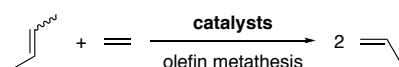


Figure 1. Amounts of products obtained at 25 °C, with **1** (3.7 μmol) and ethylene (92.0 μmol) in C₆D₆, as determined by ¹H NMR (see Supporting Information).

Remarkably, when the same experiment was conducted at 50 °C (Figure 2), this alkylidene indicator was produced in much greater amounts, reaching 24 μmol, or ca. 80% of all the organic products, at the end of the experiment (46 h),

corresponding to 6.5 turnovers,⁴¹ and demonstrating catalyzed propene formation.

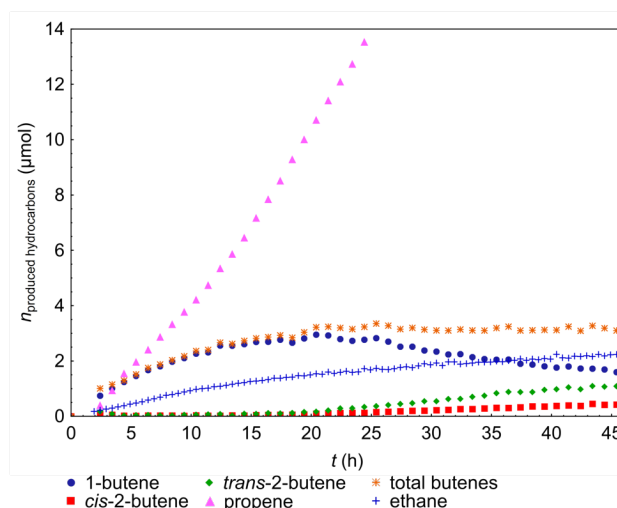


Figure 2. Amounts of products obtained at 50 °C, with **1** (3.7 μmol) and ethylene (115.0 μmol) in C₆D₆, as determined by ¹H NMR (see Supporting Information).

In an attempt to stabilize the putative Ru alkylidenes, the experiment at 25 °C was repeated in the presence of 0.6 equivalents of PCy₃. The alkylidene indicator propene again appeared alongside the same organic products as obtained without phosphine (Figure S8), but the PCy₃-stabilized alkylidenes were presumably present in too low concentrations, as suggested by the negligible amount of propene produced (e.g. 0.37 μmol after 72,3 hours), to be observed. However, when the reaction temperature was increased to 50 °C, the **GIIIm** methylidene resonance (18.42 ppm,⁴² Figure 3) started appearing in the ¹H NMR spectra two hours into the experiment. The first-generation methylidene **GII** (19.42 ppm)⁴² was also observed (albeit only transiently), as was (PCy₃)(η^6 -*p*-cymene)RuCl₂ (**2**, see Supporting Information), showing that PCy₃ may replace SIMes in **1**. Another transient Ru-alkylidene species was observed 9.5–10 h into the experiment, with a resonance (19.00 ppm) consistent with the ethylidene or propylidene analogue of **GII**.⁴³ Finally, two other weak resonances (at 18.46 and 18.38 ppm, respectively) in the alkylidene region remain unidentified.

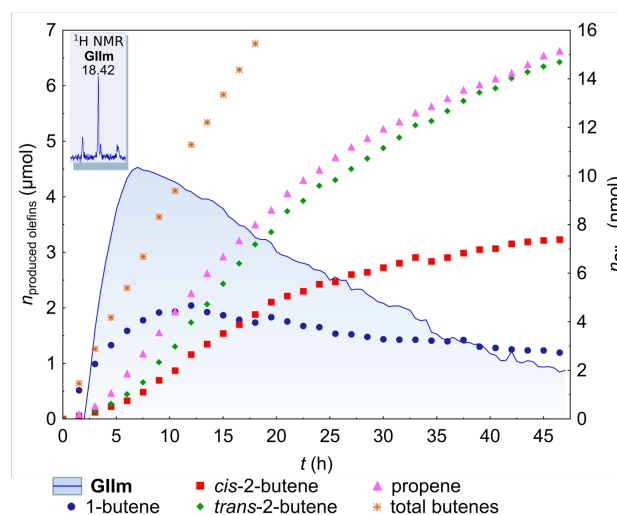


Figure 3. Amounts of C3 and C4 olefins (left ordinate) and **GIIIm** (right ordinate) obtained at 50 °C, with **1** (4.1 μmol), 0.58 equivalents of PCy₃ and ethylene (78.5 μmol) in C₆D₆, as determined by ¹H NMR (see Supporting Information). The inset shows the ¹H NMR Ru methylidene resonance recorded 7 h into the experiment. Ethane has been omitted for clarity here, but is included in Figure S12.

That **GIIIm** is formed at all is surprising given the excess of a catalyst poison (ethylene) and the fact that similar experiments have been conducted to decompose **GIIIm**.²⁶ The **GIIIm** yield attains a maximum at 7 h (10.4 nmol, 0.25%), and then declines steadily (Figure 2). Counting from this maximum, **GIIIm** decomposes at a rate (39% in 16 h) that, at first glance, is similar to that observed earlier for **GIIIm** (38% in 16 h).²⁶ However, the latter experiment was performed at a lower temperature (40 °C). Most probably, the lower temperature was compensated for by the much higher **GIIIm** concentration (0.17 M compared to less than 0.017 mM here), which ensured a larger contribution from bimolecular decomposition pathways than here.^{35,44}

Propene Formation. Whereas 1-butene is the dominating product at 25 °C (Figure 1), propene takes over at 50 °C (Figure 2). This elevated temperature is also necessary for detection of phosphine-stabilized alkylidenes (Figure 3), supporting the assumption that propene formation requires alkylidene.

Ruthenium alkylidenes can form propene by mediating ethenolysis of 2-butene (Scheme 2), a process that is particularly visible in the phosphine-free experiment at 50 °C (Figure 2). Here, propene is produced in catalytic amounts, excluding ruthenacyclobutane decomposition as the leading source. Moreover, 2-butene emerges at the very beginning, but then all but disappears for more than 20 h, during the same period in which propene is produced at an increasing rate. At this stage, any 2-butene, formed directly *via* coupling of ethylene or *via* isomerization of 1-butene, appears to be rapidly consumed by ethenolysis. One of the possible routes to propene thus involves a two-step conversion of 1-butene, which explains the falling rate with which 1-butene, the dominating product at the beginning, is formed during the first half of the experiment. In the second half, the concentration of 1-butene declines at a more constant rate. At the same time, the propene formation rate is falling and 2-butenes start to accumulate. Evidently, the latter are no longer completely consumed by ethenolysis, reflecting a lower ethylene concentration and decomposition of the active alkylidene species.

The corresponding experiment involving phosphine (50 °C, Figure 3) produces less olefins, with a total (after 47 h) of 6.7 μmol of propene and 11.0 μmol of butenes. Still, these are catalytic amounts, corresponding to 1.6 and 2.7 turnovers, respectively.⁴¹ During the first few hours, 1-butene is the dominating product, but the propene formation rate increases rapidly. At the same time, the overall butene formation rate remains approximately constant, suggesting that the C3 and C4 products are formed by different active species. The assumption that propene formation involves alkylidene can now be checked by testing whether the propene formation rate correlates with the concentration of **GIIIm**. With this being a catalytically inactive alkylidene and with more than one process leading to propene, the near-quantitative correlation in parts of Figure 4 is probably coincidental. At the more qualitative level, the correlation corroborates the involvement of Ru alkylidenes in propene formation. Looking at the details of this connection, only alkylidene decomposition can

contribute to propene formation at the very beginning of the experiment. At this stage, the rate of 2-butene ethenolysis must be zero or close to zero, since the initial concentrations of free alkylidenes and 2-butenes are all zero. Whereas in the corresponding phosphine-free experiment (Figure 2) the free alkylidenes, once formed in sufficient amount (after 2-3 h), were assumed to keep the 2-butene concentrations close to zero, these concentrations are seen to grow in the presence of PCy₃ (Figure 3). Presumably, sufficient alkylidene is trapped by PCy₃ for ethenolysis to no longer use all the 2-butene.

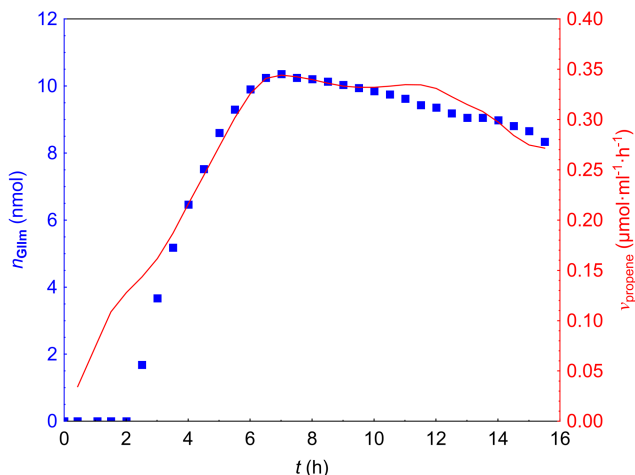


Figure 4. Yield of **GIIIm** (left ordinate, blue squares) and the propene generation rate (right ordinate, red line smoothed using the T4253H function; see Supporting Information). Prior to the smoothing, the propene generation rate was obtained by plotting the average rate of every 0.5 h interval. This average was calculated by dividing the difference between the concentration of the product (μmol·ml⁻¹) at reaction time $t + 0.5$ (h) and t (h) by the time interval 0.5 (h).

Butene Formation. Butenes are important products in the above experiments, suggesting, as discussed in the Reaction Mechanisms section below, that the *p*-cymene-free **Ru-4** or a closely related species mediates ethylene coupling. Whereas 1-butene is the dominating product at alkylidene-suppressing low temperature (25 °C, Figure 1), 2-butenes dominate at higher temperature and in the presence of the alkylidene trap PCy₃ (50 °C, Figure 3).

Although, to our knowledge, this ethylene dimerization has not been reported before, it manifests itself in metathesis experiments. For example, without the presence of alkynes or other metathesis activators, **1** and congeners thereof have been reported to cycloisomerize dienes to exo-methylene rings that are alkene coupling product analogues of 1-butene.⁴⁵⁻⁴⁸ The same reactivity has been reported for decomposed ruthenium alkylidene olefin metathesis catalysts.⁴⁹⁻⁵² For example, heating **GII** in DMF leads to loss of the alkylidene ligand. The resulting ruthenium complex, presumably similar to **1**, is an efficient cycloisomerization catalyst.⁵⁰

The alkene coupling that manifests itself as cycloisomerization when dienes are used as substrates may even take place alongside alkylidene-catalyzed metathesis, due to competing catalyst decomposition. For example, 1-butene has been observed as a prominent byproduct in reactions of **GII** and **GIIIm** with ethylene.²⁶ Since self-metathesis of propene, the organic product of the 1,2-H shift in Scheme 1, results in 2-butene, and the preferred decomposition pathway for substituted ruthenacyclobutane also produces an internal

alkene,³¹ the most likely explanation for the observed 1-butene is ethylene coupling mediated by alkylidene-free metathesis catalyst decomposition products such as to **Ru-4**.

Turning now to the butene distributions obtained in the individual experiments, 1-butene is the dominant product at low temperature (25 °C), both with (Figure S8) and without phosphine (Figure 1). Less 2-butene is produced at low temperature, and surprisingly, even though *trans*-2-butene is more stable than the *cis*-isomer, the *cis/trans* ratio remains close to unity far into these experiments. More generally, at low temperature the product yields form nearly straight lines during the first half of the experiments. In other words, the butene formation rates remain fairly constant for a long while and only appear to be influenced by isomerization in the second half of the experiments. Whereas the initial reactivity in these experiments thus could be dominated by a single active species, presumably **Ru-4** generated by dissociation of *p*-cymene from **1** (see the Reaction Mechanisms section below), the subsequent variation in formation rates is likely to originate from isomerization catalyzed by other active species generated during the experiments.

At 50 °C, isomerization is much more visible (Figure 2). The 1-butene formation rate decreases over time and even becomes negative, while those of 2-butene remain positive, suggesting that 2-butene is, at least partly, formed *via* isomerization of 1-butene. In addition, the *cis/trans* ratio falls more rapidly (to 0.38) than in the corresponding experiment at 25 °C (to 0.79). These isomerization reactions may be mediated by ruthenium hydrides: A singlet, at -11.78 ppm in the ¹H NMR spectrum appears after ca. 20 hours, and its intensity slowly increases with time, and it reaches 17.5 nmol at the end of the experiment.

Isomerization is visible also in the corresponding experiment involving phosphine (Figure 3). Here, the 1-butene yield reaches a maximum, at 13 h, coinciding with a maximum in the rate of formation of 2-butene (Figure S13), suggesting that isomerization of 1-butene is responsible for much of the 2-butene. This transformation may be catalyzed by products, potentially cyclometalated complexes³¹ or nanoparticles,³⁴ of the decomposition of both **GIm** (Figure 3) and the butene-producing species. Some resonance peaks are recorded in the hydride region of the ¹H NMR spectrum: A doublet, at -7.48 ppm (d, ²J_{PH} = 51 Hz, ¹H), in the ¹H NMR spectrum appears after ca. 10 h and reaches a maximum in intensity, corresponding to 17 nmol, after ca. 25 h, see Supporting Information for details.

Effect of Phosphine on the Reaction of 1 with Ethylene. In the above experiment at 50 °C, the trapping agent PCy₃ partly converted **1** into **2** (the PCy₃-analogue of **1**) and, to some extent, also to **GIm**. To single out the effects of phosphine, we repeated this experiment using **2** instead of **1**. Gratifyingly, although **2** gives the same organic products as **1**, only 0.25 μmol of olefins was obtained during 47 h of experiment, compared with 17.5 μmol using **1**. The activity of **2** is thus negligible and its main effect as a side product in experiments using **1** combined with PCy₃ as trapping agent is thus expected to be a mere reduction in the amount of organic products.

The low activity of **2** is partly caused by its higher stability. Whereas the ¹H NMR resonances of **1** disappear after a couple of hours, 40 % of **2** is still present at the end of the experiment (47 h). This stability also affects the generation of **GIm**, which reaches its maximum yield only very late (38 h). Although the latter yield (0.55%) is twice the maximum yield of **GIm** in the corresponding experiment using **1**, this is not reflected in more metathesis products such as propene (Scheme 2). Although

propene is, as in the experiment using **1** (Figure 3), the most abundant olefinic product, the concentration of butenes remains vanishingly low throughout the experiment. This suggests that ethenolysis of 2-butene is unimportant and that most of the propene originates from decomposition of ruthenacyclobutane.

In addition to reducing the amount of organic products by generating the less active **2**, PCy₃ also slows down the catalytic activity by coordinating to the metal center, i.e., by competing with ethylene for available coordination sites. In particular, the phosphine complexes of Ru methylidenes are known to be stable and to act as thermodynamic sinks during olefin metathesis.^{53,54} Higher phosphine concentrations should therefore lead to more **GIm** and **GIm** and less propene, since fewer 14-electron Ru alkylidenes will be available for propene formation via ethenolysis and decomposition of ruthenacyclobutanes. To test this hypothesis, we repeated the reaction of **1** at 50 °C using twice the original amount of PCy₃ (1.2 equiv.). Indeed, whereas the additional phosphine resulted in much less propene (0.7 μmol vs. 6.6 μmol with 0.6 equiv. of PCy₃) and olefins in general (>50% reduction), it resulted in much more of the first-generation catalyst. Whereas **GIm** was only observed transiently with 0.6 equiv. of PCy₃, with 1.2 equiv. of PCy₃, the concentration of this methylidene was almost three times higher (6.0 nmol, 0.17%) than that of **GIm** (2.1 nmol, 0.06%, similar to that of the 0.6 equiv. experiment) at the end of the end of the experiment (at 47 h).

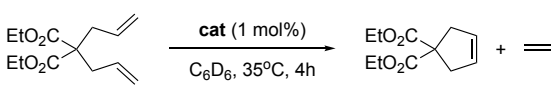
Summarizing, the presence of phosphine in the above experiment using **1** (Figure 3) does not result in organic products different from those of the corresponding phosphine-free experiment. Phosphine merely lowers the amount of such products. The additional tests described here show that PCy₃ brings about this lowering by forming the less active phosphine analogue **2** and by competing with ethylene for available sites. Some **GIm** is also formed.

The Origin of Ethane. The reduction of ethylene to ethane, a minor product in all the above experiments (see, e.g., Figure 1 and 2), is surprising as no obvious source of hydrogen is present. Grubbs-type catalysts are known to abstract hydrogen from unexpected sources such as alcohols.⁵⁵⁻⁵⁷ However, the absence of oxidized organic compounds such as acetylene and butadiene suggests that ethylene is not the hydrogen source. Moreover, the yield of ethane is always lower than the ruthenium loading (see Supporting Information for details), strongly suggesting that the reaction is stoichiometric. Thus, the most likely source of hydrogen are the two ligands SImes and PCy₃, both of which have been observed to undergo Ru-catalyzed hydrogen abstraction.^{13,33,58,59,60-62} Indeed, when the dimer [(*p*-cymene)RuCl₂]₂, from which **1** and **2** can be obtained by addition of SImes and PCy₃, respectively, is heated with ethylene at 50 °C, no ethane is observed even after six days. This experiment rules out *p*-cymene as the reductant and points at partial dehydrogenation of SImes and PCy₃ in the presence of ethylene as the most likely explanation for ethane being a product of the reactions of **1** and **2** with ethylene.

Use of 1 in Olefin Metathesis. Above we have seen that Ru methylidenes are formed on treatment of **1** with ethylene and without the use of classical carbene initiators. The mere observation of these methylidenes, along with their mechanism of formation (see below), is the emphasis of this contribution. We have not attempted to optimize the yields, which remain well below 1%. Still, to offer a glimpse of the potential future utility of the ethylene-triggered methylidene formation, we have tested **1** as catalyst for ring-closing metathesis (RCM) of

diethyl diallylmalonate (DEDAM, Table 1), both before (entry 1) and after heating in excess ethylene (entry 2). The pretreatment with ethylene (7 h in excess ethylene at 50 °C) results in nearly 20 times more RCM product.

Table 1. RCM of DEDAM Using 1.^a



entry	catalyst	conv (%) ^b	yield (%) ^b
1	1	1	1
2	1 ^c	19	19

^aConditions: catalyst: **1** (1 mol%) + 0.6 equiv. PCy₃, [DEDAM] = 0.1 M, 35 °C in C₆D₆, 4 hours. ^bDetermined by ¹H NMR analysis using 2,2,3,3-tetramethylbutane as internal standard. ^cHeated at 50 °C for 7 h in excess ethylene.

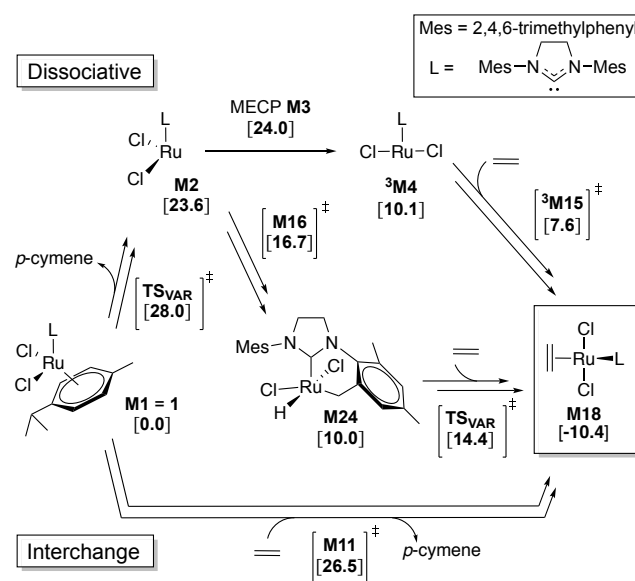
GIIm Formation: Reaction Order in Ru. In a previous investigation of the reactivity of **1** with allylbenzene, the rate of alkylidene formation was suggested, based on the observed ratio between olefin isomerization and metathesis, to be first order in **1** at high concentrations and to approach second order at low concentrations.³¹ Thus, to narrow down the computational exploration of possible mechanisms (described below), we studied the formation of **GIIm** at different concentrations of **1**. The reaction at 50 °C with 0.6 equiv. of PCy₃ (Figure 3) was repeated using a three-fold smaller and a three-fold larger amount of **1**, respectively. Next, the reaction order in ruthenium was determined using the initial rate method (Figure S22).⁶³ Although the model was based on three points only, it is clearly incompatible with an initial rate that is second order in **1**. Instead, the response in initial rate as a function of [**1**] is consistent with a reaction order below or equal to one. Mononuclear ruthenium alkene activation mechanisms are thus the focus of the below computational study.

Mechanistic Density Functional Theory (DFT) Study. The mechanisms of formation of both ruthenium alkylidenes and organic products have been investigated using DFT. The functional, basis sets, and further details of the computational model are defined in the Computational Details section of the Supporting Information. Whereas the Supporting Information also contains all the computational results, including structures and energies of unfavored reaction pathways and intermediates, the following presentation summarizes the most probable and important parts of the reaction network.

In the DFT calculations, the role of PCy₃ has been limited to that of “trapping” alkylidenes such as **GIIm**. As we have seen above, the same organic products are obtained with and without PCy₃. Although the kinetics of formation of these organic products is influenced by the presence of phosphine, this influence appears, as discussed above, to mainly involve catalyst deactivation via PCy₃ coordination and, importantly, NHC/PCy₃ exchange in **1** to form the less reactive **2**. Thus, when phosphine is added, the observed activity will be lower and due to both **1** and **2**, with the contribution from **2** increasing during the experiment. Since **2** predominantly produces propene, **GIIm**, and ethane (see above and the Supporting Information), addition of PCy₃ in experiments with **1** will progressively give less butene than the corresponding phosphine-free experiments. Summarizing, **1** and **2** give the same kinds of products, but **1** has a richer reactivity, and this reactivity is the one studied in the following.

Mechanistic DFT Study: Alkylidene and Propene Formation. First, the reactivity of **1** toward ethylene is evident already from the remarkable stability of ethylene complex **M18** (Scheme 3). Despite being a 14-electron complex, **M18** is more than 10 kcal/mol more stable than the 18-electron **M1**. However, substitution of *p*-cymene by ethylene in **M1** requires more than 25 kcal/mol of activation. The calculations favor, albeit by a small margin (1.5 kcal/mol), an interchange mechanism in which ethylene binds at the same time as *p*-cymene dissociates. In the case of a purely dissociative mechanism, which is likely to be favored for bigger substrates than ethylene,³¹ the electron deficient intermediate **M2** will seek stabilization either by undergoing spin inversion to the spin-triplet ³**M4** or by coordinating and inserting into a methyl C–H bond of a SIMes mesityl substituent to form **M24**. While both ³**M4** and **M24** are efficient olefin isomerization catalysts (see Supporting Information and ref³¹) that may contribute to the above-described diversity of organic products, both are also 10 kcal/mol less stable than **M1**. Hence, as long as enough ethylene is present, ³**M4** and **M24** will readily bind this substrate to form the more than 20 kcal/mol more stable **M18**. The latter ethylene complex plays a pivotal role in the reaction network described in the following.

Scheme 3. Activation of **1** = **M1** by exchange of *p*-cymene with ethylene.^a



^a**M1** is the computational model of compound **1**. Free energies at 25 °C are reported in kcal/mol relative to **M1**. Variational transition states (TS_{VAR}) offer lower-bound estimates of the barrier for elementary steps assumed to be diffusion controlled. The energy reported here for **M3**, the minimum energy crossing point (MECP) between the spin-singlet **M2** and the spin-triplet ³**M4**, is the lower-bound estimate. See Supporting Information for computational details and the complete mechanism.

Even if **M18** is stable relative to **M1**, it readily binds a second ethylene molecule and several bis-η²-olefin complexes may be formed. A complex (**M50**, cf. Supporting Information) in which the two C=C bonds are nearly orthogonal to each other is the most stable, at -12.2 kcal/mol, but is not reactive. In contrast, the nearly parallel orientation in **M47** (Scheme 4) ensures a surprisingly facile oxidative coupling, with a <8 kcal/mol barrier relative to **M47**, to reach the more stable

ruthenacyclopentane **M49**. As shown already,³¹ **M49** can undergo formal 1,2- or 1,3-H shifts. While a high-barrier 1,3-H shift leads directly to 1-butene (see Supporting Information), the preferred, low-energy pathway is more indirect. The first step on this pathway is β -H elimination and gives a Ru-hydride decorated by a chelating, η^2 -coordinated butenyl ligand (**M55**). **M55** is a junction from which two main branches in the subsequent reaction network extends (Scheme 4).

In the first of these branches, **M55** may complete the 1,2-H shift started in **M49** and obtain, in a reaction that is the reverse of the metallacyclobutane ring expansion studied in ref ³¹, bottom-bound⁶⁴ methyl-substituted metallacyclobutane **M303** *via* transition state **M302**. Importantly, the ruthenacyclobutane **M303** may collapse to give either 14-electron Ru methylidene **M309** and propene or 14-electron Ru ethylidene **M312** and ethylene. The barriers from **M303** estimated for the two collapses are very similar, 11.1 (*via* transition state **M307**) and 11.2 kcal/mol (assumed to occur *via* a variational transition state, since no transition state on the potential energy surface could be found) for methylidene and ethylidene formation, respectively. However, the latter barrier is a lower-bound estimate (cf. Supporting Information) and the calculations are thus consistent with Figure 3 and the above-described experiments: **GIIIm**, the molecular model of which is **M310**, is the main Ru alkylidene observed, while ethylidene **M312** may be among the transiently observed alkylidenes.

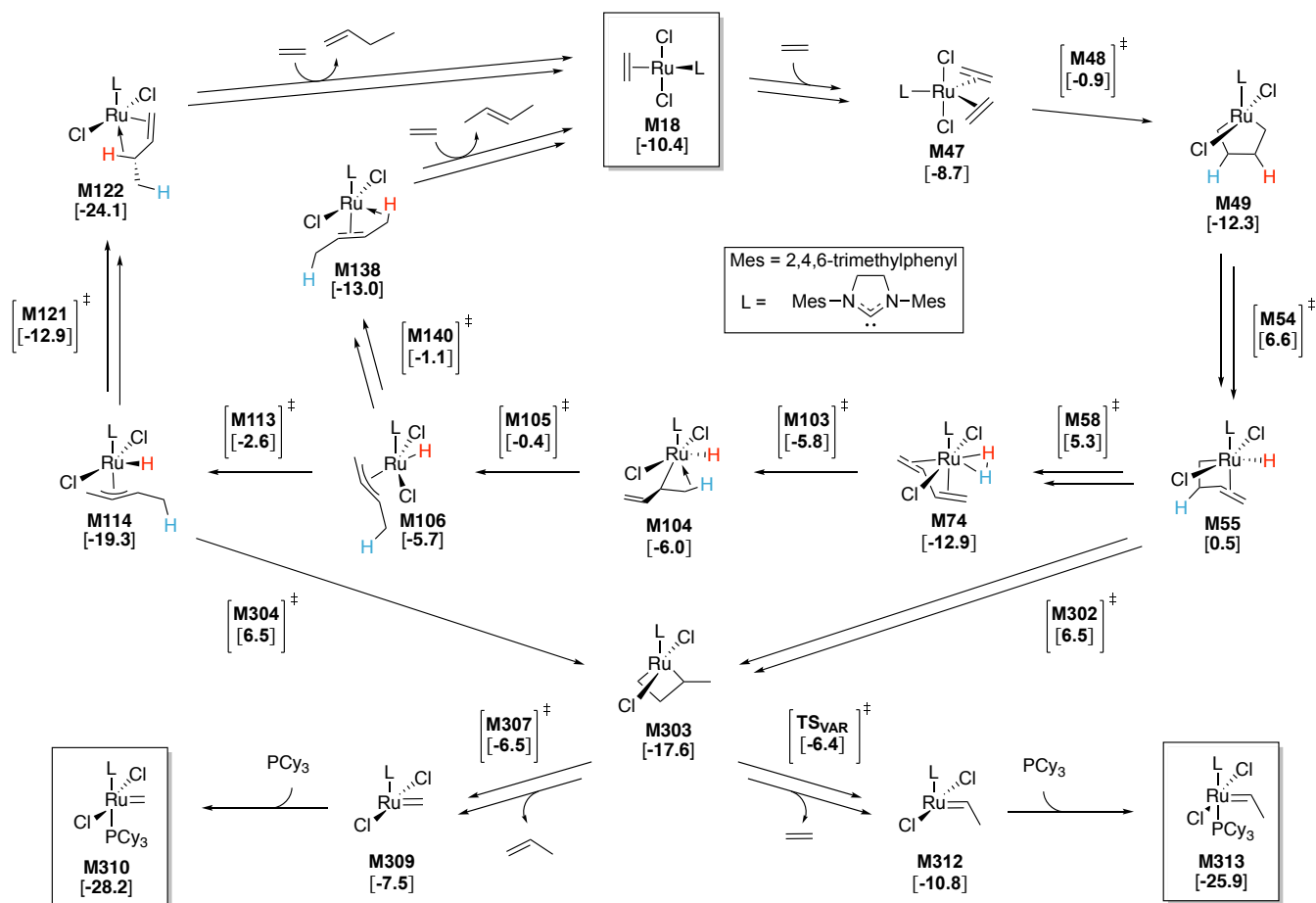
Concluding, this, the first branch continuing from **M55**, explains the formation of the observed **GIIIm** from **1** and also shows that propene is liberated alongside **GIIIm**, i.e., propene is an indicator of Ru methylidene generation and not only decomposition as in Scheme 1. This implies that part of the propene observed at the beginning of experiments performed at 50 °C (Figures 3 and 4) stems from generation of alkylidenes *via* a stoichiometric process. This process thus adds to propene

Scheme 4. Mechanism for the catalytic coupling of ethylene to form 1-butene and *trans*-2-butene, with off-cycle formation of propene and phosphine-stabilized alkylidene.^a

generated via the already assumed contributions from ethenolysis of 2-butene (catalytic) and alkylidene decomposition (stoichiometric).

Mechanistic DFT Study: Butene Formation. From the above-mentioned junction **M55**, the second branch runs *via* transition state **M58** and predicts fast formation of 1-butene and slow formation of *trans*-2-butene (Scheme 4). This pathway is populated by several η^3 -allylic Ru-hydrides (e.g., **M114**) that could rearrange to reach (e.g., *via* transition state **M304**) the methyl-substituted ruthenacyclobutane **M303** of the first, alkylidene-producing branch. Whereas this kind of reactivity has been suggested for the initiation of alkylidene-free tungsten-based metathesis catalysts,^{65,66} the path *via* **M304** and similar alternatives connecting the η^3 -allylic Ru-hydrides to **M303** are more energy-demanding than the pathways leading to 1- and 2-butene (see Supporting Information).

Most importantly, the energy barriers discriminating between the two branches, involving transition states **M302**, **M58** and rate-determining intermediate **M49**, are 18.8 and 17.6 kcal/mol, respectively. The latter path, *via* **M58**, is thus favored, predicting that formation of butenes requires less activation than that of propene and alkylidenes. This prediction can be tested by comparing the rates of butene and propene formation at the beginning of the experiments, when alkylidenes are absent and ethenolysis of 2-butene and decomposition of unsubstituted ruthenacyclobutane (Scheme 1) do not contribute much to propene formation. Thus, at the very beginning of an experiment, any propene observed must stem mainly from cycloreversion of **M303**, which, according to the calculations, should be slower than butene formation *via* **M58**. Indeed, the initial 1-butene formation rate is higher than that of propene in all our experiments (see, e.g., Figure 1, 2 and 3), thus corroborating the mechanism presented in Scheme 4.



^aFree energies at 25 °C are reported in kcal/mol relative to **M1** only for the most important intermediates and the rate- and product-determining transition states. For computational details and the complete mechanism, see the Supporting Information. Although conformational flexibility at **M74** suggests that the two H atoms of dihydrogen are equivalent (i.e., scrambled), they are labeled by color (red, blue) to help convey the mechanism.

Turning now to the details of the complex branch running *via* **M58**, butene formation starts by dissociation of the metal-alkene bond in **M55**. Instead, the metal atom forms a β -H agostic interaction (see Supporting Information). The subsequent β -H elimination leads to a Ru center coordinated by butadiene and σ -bound molecular hydrogen (**M74**). Liberation of either butadiene or hydrogen is markedly endergonic and predicted to be unlikely, consistent with the lack of observation of these products in the above experiments. Instead, one of the hydrogen atoms of the H₂ ligand is transferred back to the end of the C4 fragment, creating the butenyl ligand in **M104**. The latter can be bent to give the η^3 -allylic hydride complex **M106**.

In **M106** the η^3 -allylic ligand is essentially *trans* to the remaining hydride ligand, which thus may be transferred to either end of the allylic C3 fragment. This flexibility means that, from **M106**, both *trans*-2-butene (*via* transition state **M138**) and 1-butene (*via* transition state **M113**) may be formed. Formation of 1-butene is kinetically favored by 1.5 kcal/mol. This preference is consistently reproduced by different DFT methods (see Supporting Information) and agrees with the experimentally observed faster initial, i.e., prior to potential influence of isomerization, formation of 1-butene than of *trans*-2-butene (Figures 1-3). Finally, the butene release, which most likely occurs *via* associative exchange or interchange with ethylene (see Supporting Information), regenerates the Ru(II) species **M18** and concludes the catalytic cycle leading to 1-butene and *trans*-2-butene.

Turning now to the origin of *cis*-2-butene, the variation in formation rates for *cis*- and *trans*-2-butene as well as for 1-butene at 50 °C, especially in the presence of phosphine (Figure 3), suggest that isomerization of 1-butene to 2-butene and of *cis*- to *trans*-2-butene contributes at higher temperatures. In contrast, at room temperature the similar and fairly constant *cis*- and *trans*-2-butene formation rates (Figure 1), which do not reflect the thermodynamic stability of these two olefins, suggest direct formation of both *cis* and *trans*-2-butene (as seen in Scheme 4) and rate laws that are independent of the 1-butene concentration. This is consistent with the fact that none of the many 1- and 2-butene isomerization pathways that were explored computationally (see Supporting Information) could explain the similar and near-constant formation rates for the two 2-butene isomers at room temperature.

Thus, we have also explored many candidate pathways for direct formation of *cis*-2-butene from ethylene, but none of these are consistent with this isomer forming at a rate similar to that of the *trans*-isomer. The most likely explanation for the formation of *cis*-2-butene early on in the experiments (Figure 1) is an alternative, so far unidentified, pathway. We speculate that, since the pathway to *trans*-2-butene in Scheme 4 involves an *s-trans* butadiene at **M74** and a *syn* η^3 -allyl species **M106**, an analogous reaction involving *s-cis*-butadiene and *anti* η^3 -allylic ligand would generate *cis*-2-butene. In fact, barriers for the key hydride transfer reactions of a Ru-bound *s-cis*-butadiene complex were found to be lower than those of the

corresponding *s-trans* complex (see Supporting Information), but the *s-cis*-butadiene complex could so far not be connected to the rest of the reaction network with sufficiently low barriers to be competitive.

Apart from this lack of connection in the *cis*-formation pathway, the calculations reflect the experiments and offer mechanistic explanations for all the key observations: The fact that 1-butene is the first and major product at low temperatures and the somewhat slower formation of 2-butene, the promoting effect of temperature on the alkylidene formation, and the intimate connection between alkylidene and propene formation. This ruthenium alkylidene marker is, according to the calculations, released stoichiometrically both during methylidene formation and decomposition. Once alkylidene has been formed, propene is also produced catalytically *via* ethenolysis of 2-butene.

CONCLUSIONS

We have shown that ruthenium methylidenes **GII**m and **GII**m form on reaction of PCy₃ and ethylene, a known ruthenium alkylidene metathesis catalyst poison, with **1**. Since **1** is closely associated with compounds resulting from loss of alkylidene from Grubbs-type metathesis catalysts, these results imply that catalyst decomposition *via* alkylidene loss is, contrary to long-standing beliefs, reversible.

Importantly, the reversibility might be utilized to achieve Ru alkylidene metathesis catalysts with higher turnover numbers by promoting, *via* catalyst or process design, continuous alkylidene regeneration from decomposition product analogues of **1** during catalysis. Indeed, pretreatment of **1** with ethylene resulted in an almost 20-fold increase in activity for ring-closing metathesis of DEDAM. Similarly, insight into benign routes from **1** and analogues thereof to Ru alkylidenes may also be used to circumvent the expensive and explosive diazo technology used to install the benzylidene ligand of catalysts such as **GII**.⁶⁷

Mechanistic DFT calculations suggest that the connection between **1** and **GII**m, the main methylidene formed, starts by ethylene replacing *p*-cymene in **1** (= **M1**) *via* an interchange mechanism. The resulting ethylene complex **M18** can readily bind a second ethylene and undergo oxidative coupling to form metallacyclopentane **M49**. From **M49** a 1,2-H shift leads to methyl-substituted ruthenacyclobutane **M303**, followed by cycloreversion and propene release to give the 14-electron methylidene **Ru-1** (= **M309**) that may be trapped by PCy₃ as **GII**m (= **M310**). This mechanism implies that propene release is intimately connected not only to decomposition of metallacyclobutane **Ru-2** (Scheme 1) and ethenolysis of 2-butene (Scheme 2), but also to formation of **GII**m itself.

The reaction of **1** with ethylene produces catalytic amounts of propene and butenes. Whereas propene and **GII**m require some time to form and are also promoted by higher temperature, the first and dominating product, in particular at lower temperature, is 1-butene. This is also reflected in the calculations, which predict a lower barrier to butene formation than to formation of Ru alkylidene as well as faster formation of 1-butene than of 2-butene.

ASSOCIATED CONTENT

Supporting Information

The Supporting Information is available free of charge on the ACS Publications website at DOI: xxxxx. Experimental methods, additional results and data from

catalytic tests, NMR spectra, computational methods, additional computational results, validation of computational models, and sample input files (PDF), calculated molecular models (XYZ).

AUTHOR INFORMATION

Corresponding Author

* Marco.Foscatto@uib.no, Giovanni.Occhipinti@uib.no, Vidar.Jensen@uib.no

Author Contributions

#These authors contributed equally.

Notes

The authors declare no competing financial interests.

ACKNOWLEDGMENT

This work was funded by the Research Council of Norway (RCN, *via* project 262370, the Norwegian NMR Platform, 226244, CPU and storage resources granted through the NOTUR (NN2506K) and NORSTORE (NS2506K) projects). WS is grateful for a PhD studentship from the University of Bergen.

REFERENCES

- (1) *Handbook of metathesis*; 2nd ed.; Grubbs, R. H.; Wenzel, A. G.; O'Leary, D. J.; Khosravi, E., Eds.; Wiley-VCH: Weinheim, 2015; Vol. 1-3.
- (2) Scholl, M.; Ding, S.; Lee, C. W.; Grubbs, R. H. Synthesis and activity of a new generation of ruthenium-based olefin metathesis catalysts coordinated with 1,3-dimesityl-4,5-dihydroimidazol-2-ylidene ligands, *Org. Lett.* **1999**, *1*, 953-56.
- (3) Farina, V.; Horváth, A. In *Handbook of Metathesis*; 2nd ed.; Grubbs, R. H., Wenzel, A. G., O'Leary, D. J., Khosravi, E., Eds.; Wiley-VCH: Weinheim, 2015; Vol. 2, p 633-58.
- (4) Higman, C. S.; Lummiss, J. A. M.; Fogg, D. E. Olefin Metathesis at the Dawn of Implementation in Pharmaceutical and Specialty-Chemicals Manufacturing, *Angew. Chem. Int. Ed.* **2016**, *55*, 3552-65.
- (5) Stoianova, D.; Johns, A.; Pederson, R. In *Handbook of Metathesis*; 2nd ed.; Grubbs, R. H., Wenzel, A. G., O'Leary, D. J., Khosravi, E., Eds.; Wiley-VCH: Weinheim, 2015; Vol. 2, p 699-726.
- (6) Goudreaux, A. Y.; Walden, D. M.; Nascimento, D. L.; Botti, A. G.; Steinmann, S. N.; Michel, C.; Fogg, D. E. Hydroxide-Induced Degradation of Olefin Metathesis Catalysts: A Challenge for Metathesis in Alkaline Media, *ACS Catalysis* **2020**, 3838-43.
- (7) Maechling, S.; Zaja, M.; Blechert, S. Unexpected Results of a Turnover Number (TON) Study Utilising Ruthenium-Based Olefin Metathesis Catalysts, *Adv. Synth. Catal.* **2005**, *347*, 1413-22.
- (8) Conrad, J. C.; Fogg, D. E. Ruthenium-catalyzed ring-closing metathesis: Recent advances, limitations and opportunities, *Curr. Org. Chem.* **2006**, *10*, 185-202.
- (9) du Toit, J. I.; van der Gryp, P.; Loock, M. M.; Tole, T. T.; Marx, S.; Jordaan, J. H. L.; Vosloo, H. C. M. Industrial viability of homogeneous olefin metathesis: Beneficiation of linear alpha olefins with the diphenyl-substituted pyridinyl alcoholato ruthenium carbene precatalyst, *Catal. Today* **2016**, *275*, 191-200.
- (10) Higman, C. S.; Lanterna, A. E.; Marin, M. L.; Scaiano, J. C.; Fogg, D. E. Catalyst Decomposition during Olefin Metathesis Yields Isomerization-Active Ruthenium Nanoparticles, *ChemCatChem* **2016**, *8*, 2446-49.
- (11) Schrodi, Y.; Ung, T.; Vargas, A.; Mkrtumyan, G.; Lee, C. W.; Champagne, T. M.; Pederson, R. L.; Hong, S. H. Ruthenium Olefin Metathesis Catalysts for the Ethenolysis of Renewable Feedstocks, *Clean: Soil, Air, Water* **2008**, *36*, 669-73.
- (12) Nickel, A.; Ung, T.; Mkrtumyan, G.; Uy, J.; Lee, C. W.; Stoianova, D.; Papazian, J.; Wei, W.-H.; Mallari, A.; Schrodi, Y.; Pederson, R. L. A Highly Efficient Olefin Metathesis Process for the Synthesis of Terminal Alkenes from Fatty Acid Esters, *Top. Catal.* **2012**, *55*, 518-23.
- (13) Hong, S. H.; Wenzel, A. G.; Salguero, T. T.; Day, M. W.; Grubbs, R. H. Decomposition of ruthenium olefin metathesis catalysts, *J. Am. Chem. Soc.* **2007**, *129*, 7961-68.

- (14) Wyrębek, P.; Małecki, P.; Sytniczuk, A.; Kośnik, W.; Gawin, A.; Kostorzewa, J.; Kajetanowicz, A.; Grela, K. Looking for the Noncyclic(amino)(alkyl)carbene Ruthenium Catalyst for Ethenolysis of Ethyl Oleate: Selectivity Is on Target, *ACS Omega* **2018**, *3*, 18481-88.
- (15) Biermann, U.; Bornscheuer, U.; Meier, M. A. R.; Metzger, J. O.; Schafer, H. J. Oils and Fats as Renewable Raw Materials in Chemistry, *Angew. Chem. Int. Ed.* **2011**, *50*, 3854-71.
- (16) Chikkali, S.; Mecking, S. Refining of Plant Oils to Chemicals by Olefin Metathesis, *Angew. Chem. Int. Ed.* **2012**, *51*, 5802-08.
- (17) Kajetanowicz, A.; Chwalba, M.; Gawin, A.; Tracz, A.; Grela, K. Non-Glovebox Ethenolysis of Ethyl Oleate and FAME at Larger Scale Utilizing a Cyclic (Alkyl)(Amino)Carbene Ruthenium Catalyst, *European Journal of Lipid Science and Technology* **2020**, *122*, 1900263.
- (18) Hong, S. H.; Day, M. W.; Grubbs, R. H. Decomposition of a Key Intermediate in Ruthenium-Catalyzed Olefin Metathesis Reactions, *J. Am. Chem. Soc.* **2004**, *126*, 7414-15.
- (19) McClellan, W. L.; Ruff, S. A.; Lummiss, J. A. M.; Fogg, D. E. A General Decomposition Pathway for Phosphine-Stabilized Metathesis Catalysts: Lewis Donors Accelerate Methylidene Abstraction, *J. Am. Chem. Soc.* **2016**, *138*, 14668-77.
- (20) Poater, A.; Ragone, F.; Correa, A.; Cavallo, L. Exploring the Reactivity of Ru-Based Metathesis Catalysts with a π -Acid Ligand Trans to the Ru–Ylidene Bond, *J. Am. Chem. Soc.* **2009**, *131*, 9000-06.
- (21) Poater, A.; Cavallo, L. Deactivation of Ru-benzylidene Grubbs catalysts active in olefin metathesis, *Theor. Chem. Acc.* **2012**, *131*, 1155.
- (22) Tsang, W. C. P.; Schrock, R. R.; Hoveyda, A. H. Evaluation of Enantiomerically Pure Binaphthol-Based Molybdenum Catalysts for Asymmetric Olefin Metathesis Reactions that Contain 3,3'-Diphenyl- or 3,3'-Dimesityl-Substituted Binaphtholate Ligands. Generation and Decomposition of Unsubstituted Molybdacyclobutane Complexes, *Organometallics* **2001**, *20*, 5658-69.
- (23) Leduc, A.-M.; Salameh, A.; Soulivong, D.; Chabanas, M.; Basset, J.-M.; Copéret, C.; Solans-Monfort, X.; Clot, E.; Eisenstein, O.; Böhm, V. P. W.; Röper, M. β -H Transfer from the Metallacyclobutane: A Key Step in the Deactivation and Byproduct Formation for the Well-Defined Silica-Supported Ruthenium Alkylidene Alkene Metathesis Catalyst, *J. Am. Chem. Soc.* **2008**, *130*, 6288-97.
- (24) Schrodi, Y. In *Handbook of Metathesis*; Grubbs, R. H., Wenzel, A. G., O'Leary, D. J., Khosravi, E., Eds.; Wiley-VCH: Weinheim; 2015; Vol. 1, p 323-42.
- (25) Solans-Monfort, X.; Copéret, C.; Eisenstein, O. Shutting Down Secondary Reaction Pathways: The Essential Role of the Pyrrolyl Ligand in Improving Silica Supported d^0 -ML₄ Alkene Metathesis Catalysts from DFT Calculations, *J. Am. Chem. Soc.* **2010**, *132*, 7750-57.
- (26) Janse van Rensburg, W.; Steynberg, P. J.; Meyer, W. H.; Kirk, M. M.; Forman, G. S. DFT Prediction and Experimental Observation of Substrate-Induced Catalyst Decomposition in Ruthenium-Catalyzed Olefin Metathesis, *J. Am. Chem. Soc.* **2004**, *126*, 14332-33.
- (27) Romero, P. E.; Piers, W. E. Direct observation of a 14-electron ruthenacyclobutane relevant to olefin metathesis, *J. Am. Chem. Soc.* **2005**, *127*, 5032-33.
- (28) Janse van Rensburg, W.; Steynberg, P. J.; Kirk, M. M.; Meyer, W. H.; Forman, G. S. Mechanistic comparison of ruthenium olefin metathesis catalysts: DFT insight into relative reactivity and decomposition behavior, *J. Organomet. Chem.* **2006**, *691*, 5312-25.
- (29) Romero, P. E.; Piers, W. E. Mechanistic studies on 14-electron ruthenacyclobutanes: Degenerate exchange with free ethylene, *J. Am. Chem. Soc.* **2007**, *129*, 1698-704.
- (30) Ashworth, I. W.; Hillier, I. H.; Nelson, D. J.; Percy, J. M.; Vincent, M. A. Searching for the Hidden Hydrides: The Competition between Alkene Isomerization and Metathesis with Grubbs Catalysts, *Eur. J. Org. Chem.* **2012**, *2012*, 5673-77.
- (31) Engel, J.; Smit, W.; Foscatto, M.; Occhipinti, G.; Törnroos, K. W.; Jensen, V. R. Loss and Reformation of Ruthenium Alkylidene: Connecting Olefin Metathesis, Catalyst Deactivation, Regeneration, and Isomerization, *J. Am. Chem. Soc.* **2017**, *139*, 16609-19.
- (32) Liu, P.; Taylor, B. L. H.; Garcia-Lopez, J.; Houk, K. N. In *Handbook of Metathesis*; 2nd ed.; Grubbs, R. H., Wenzel, A. G., O'Leary, D. J., Khosravi, E., Eds.; Wiley-VCH: Weinheim, 2015; Vol. 1, p 199-252.
- (33) Bailey, G. A.; Lummiss, J. A. M.; Foscatto, M.; Occhipinti, G.; McDonald, R.; Jensen, V. R.; Fogg, D. E. Decomposition of Olefin Metathesis Catalysts by Brønsted Base: Metallacyclobutane Deprotonation as a Primary Deactivating Event, *J. Am. Chem. Soc.* **2017**, *139*, 16446-49.
- (34) Higman, C. S.; Lanterna, A. E.; Marin, M. L.; Scaiano, J. C.; Fogg, D. E. Catalyst Decomposition during Olefin Metathesis Yields Isomerization-Active Ruthenium Nanoparticles, *ChemCatChem* **2016**, *8*, 2424-24.
- (35) Bailey, G. A.; Foscatto, M.; Higman, C. S.; Day, C. S.; Jensen, V. R.; Fogg, D. E. Bimolecular Coupling as a Vector for Decomposition of Fast-Initiating Olefin Metathesis Catalysts, *J. Am. Chem. Soc.* **2018**, *140*, 6931-44.
- (36) Ahr, M.; Thieuleux, C.; Copéret, C.; Fenet, B.; Basset, J.-M. Noels' vs. Grubbs' Catalysts: Evidence for One Unique Active Species for Two Different Systems!, *Adv. Synth. Catal.* **2007**, *349*, 1587-91.
- (37) Day, C. S.; Fogg, D. E. High-Yield Synthesis of a Long-Sought, Labile Ru-NHC Complex and Its Application to the Concise Synthesis of Second-Generation Olefin Metathesis Catalysts, *Organometallics* **2018**, *37*, 4551-55.
- (38) Kabro, A.; Roisnel, T.; Fischmeister, C.; Bruneau, C. Ruthenium-Indenylidene Olefin Metathesis Catalyst with Enhanced Thermal Stability, *Chem. Eur. J.* **2010**, *16*, 12255-61.
- (39) Jimenez, L. R.; Gallon, B. J.; Schrodi, Y. A Most Convenient and Atom-Economic Preparation of a Highly Active Ring-Closing Metathesis Catalyst, *Organometallics* **2010**, *29*, 3471-73.
- (40) Methane and higher olefins were not detected.
- (41) Calculated as the molar yield of the product divided by the initial molar number of 1.
- (42) Lummiss, J. A. M.; Beach, N. J.; Smith, J. C.; Fogg, D. E. Targeting an Achilles heel in olefin metathesis: A strategy for high-yield synthesis of second-generation Grubbs methylidene catalysts, *Catal. Sci. Technol.* **2012**, *2*, 1630-32.
- (43) Williams, J. E.; Harner, M. J.; Sponsler, M. B. Ruthenium Alkylidenes: Fast Initiators for Olefin Metathesis, *Organometallics* **2005**, *24*, 2013-15.
- (44) Ulman, M.; Grubbs, R. H. Ruthenium carbene-based olefin metathesis initiators: Catalyst decomposition and longevity, *J. Org. Chem.* **1999**, *64*, 7202-07.
- (45) Sémeril, D.; Bruneau, C.; Dixneuf, P. H. Ruthenium Catalyst Dichotomy: Selective Catalytic Diene Cycloisomerization or Metathesis, *Helv. Chim. Acta* **2001**, *84*, 3335-41.
- (46) Lo, C.; Cariou, R.; Fischmeister, C.; Dixneuf, P. H. Simple ruthenium precatalyst for the synthesis of stilbene derivatives and ring-closing metathesis in the presence of styrene initiators, *Adv. Synth. Catal.* **2007**, *349*, 546-50.
- (47) Lübke, C.; Dumrath, A.; Neumann, H.; Beller, M.; Kadyrov, R. Lewis Acid Assisted Ruthenium-Catalyzed Metathesis Reactions, *ChemCatChem* **2014**, *6*, 105-08.
- (48) Lübke, C.; Dumrath, A.; Neumann, H.; Schäffer, M.; Zimmermann, R.; Beller, M.; Kadyrov, R. How Important are Impurities in Catalysis? An Example from Ring-Closing Metathesis, *ChemCatChem* **2014**, *6*, 684-88.
- (49) Schmidt, B. Ruthenium-Catalyzed Cyclizations: More than Just Olefin Metathesis!, *Angew. Chem. Int. Ed.* **2003**, *42*, 4996-99.
- (50) Mallagaray, Á.; Mohammadiannejad-Abbasabadi, K.; Medina, S.; Domínguez, G.; Pérez-Castells, J. Cycloisomerization of dienes and enynes catalysed by a modified ruthenium carbene species, *Org. Biomol. Chem.* **2012**, *10*, 6665-72.
- (51) Connon, S. J.; Blechert, S. A solid-Supported phosphine-free ruthenium alkylidene for olefin metathesis in methanol and water, *Bioorg. Med. Chem. Lett.* **2002**, *12*, 1873-76.
- (52) Lexer, C.; Burtcher, D.; Perner, B.; Tzur, E.; Lemcoff, N. G.; Slugovc, C. Olefin metathesis catalyst bearing a chelating phosphine ligand, *J. Organomet. Chem.* **2011**, *696*, 2466-70.
- (53) Sanford, M. S.; Love, J. A.; Grubbs, R. H. Mechanism and activity of ruthenium olefin metathesis catalysts, *J. Am. Chem. Soc.* **2001**, *123*, 6543-54.
- (54) Lummiss, J. A. M.; Perras, F. A.; McDonald, R.; Bryce, D. L.; Fogg, D. E. Sterically Driven Olefin Metathesis: The Impact of Alkylidene Substitution on Catalyst Activity, *Organometallics* **2016**, *35*, 691-98.
- (55) Manzini, S.; Poater, A.; Nelson, D. J.; Cavallo, L.; Slawin, A. M. Z.; Nolan, S. P. Insights into the Decomposition of Olefin Metathesis Precatalysts, *Angew. Chem. Int. Ed.* **2014**, *53*, 8995-99.
- (56) Dinger, M. B.; Mol, J. C. Degradation of the First-Generation Grubbs Metathesis Catalyst with Primary Alcohols, Water, and Oxygen. Formation and Catalytic Activity of Ruthenium(II) Monocarbonyl Species, *Organometallics* **2003**, *22*, 1089-95.
- (57) Dinger, Maarten B.; Mol, Johannes C. Degradation of the Second-Generation Grubbs Metathesis Catalyst with Primary Alcohols and Oxygen – Isomerization and Hydrogenation Activities of Monocarbonyl Complexes, *Eur. J. Inorg. Chem.* **2003**, *2003*, 2827-33.

- (58) Courchay, F. C.; Sworen, J. C.; Ghiviriga, I.; Abboud, K. A.; Wagener, K. B. Understanding structural isomerization during ruthenium-catalyzed olefin metathesis: A deuterium labeling study, *Organometallics* **2006**, *25*, 6074-86.
- (59) Trnka, T. M.; Morgan, J. P.; Sanford, M. S.; Wilhelm, T. E.; Scholl, M.; Choi, T. L.; Ding, S.; Day, M. W.; Grubbs, R. H. Synthesis and activity of ruthenium alkylidene complexes coordinated with phosphine and N-heterocyclic carbene ligands, *J. Am. Chem. Soc.* **2003**, *125*, 2546-58.
- (60) Six, C.; Gabor, B.; Görls, H.; Mynott, R.; Philipps, P.; Leitner, W. Inter- and Intramolecular Thermal Activation of sp^3 C-H Bonds with Ruthenium Bisallyl Complexes, *Organometallics* **1999**, *18*, 3316-26.
- (61) Christ, M. L.; Sabo-Etienne, S.; Chaudret, B. Highly Selective Dehydrogenative Silylation of Ethylene Using the Bis(dihydrogen) Complex $RuH_2(H_2)_2(PCy_3)_2$ as Catalyst Precursor, *Organometallics* **1995**, *14*, 1082-84.
- (62) Cannon, J. S.; Zou, L.; Liu, P.; Lan, Y.; O'Leary, D. J.; Houk, K. N.; Grubbs, R. H. Carboxylate-Assisted $C(sp^3)$ -H Activation in Olefin Metathesis-Relevant Ruthenium Complexes, *J. Am. Chem. Soc.* **2014**, *136*, 6733-43.
- (63) Casado, J.; Lopez-Quintela, M. A.; Lorenzo-Barral, F. M. The initial rate method in chemical kinetics: Evaluation and experimental illustration, *J. Chem. Educ.* **1986**, *63*, 450.
- (64) Poater, A.; Cavallo, L. A comprehensive study of olefin metathesis catalyzed by Ru-based catalysts, *Beilstein J. Org. Chem.* **2015**, *11*, 1767-80.
- (65) Chan, K. W.; Lam, E.; D'Anna, V.; Allouche, F.; Michel, C.; Safonova, O. V.; Sautet, P.; Copéret, C. C-H Activation and Proton Transfer Initiate Alkene Metathesis Activity of the Tungsten(IV)-Oxo Complex, *J. Am. Chem. Soc.* **2018**, *140*, 11395-401.
- (66) Chan, K. W.; Mance, D.; Safonova, O. V.; Copéret, C. Well-Defined Silica-Supported Tungsten(IV)-Oxo Complex: Olefin Metathesis Activity, Initiation, and Role of Brønsted Acid Sites, *J. Am. Chem. Soc.* **2019**, *141*, 18286-92.
- (67) Boeda, F.; Clavier, H.; Nolan, S. P. Ruthenium-indenylidene complexes: powerful tools for metathesis transformations, *Chem. Commun.* **2008**, 2726-40.

Table of Contents Artwork

